JOURNAL OF CATALYSIS 138, 12–23 (1992)

Mechanism of Alkali and Alkaline Earth Catalyzed Gasification of Graphite by CO_2 and H_2O Studied by Electron Microscopy

S. G. CHEN AND R. T. YANG[1]

Department of Chemical Engineering, State University of New York at Buffalo, Buffalo, New York, 14260

Received February 24, 1992; revised May 26, 1992

The kinetics and mechanism of graphite gasification by CO_2 and H_2O catalyzed by five alkali and alkaline earth metal catalysts are investigated by studying the monolayer channeling action on the basal plane of graphite. CO_2 and H_2O are dissociatively chemisorbed by these catalysts, followed by diffusion of O atoms/ions to the edge carbon sites, where breakage of C–C bonds takes place to free CO. The C–C bond breakage is the rate-limiting step. The catalytic activities as measured by the turnover frequencies on the edge carbon sites follow the order K > Ba > Ca > Na > Li. The same catalytic mechanism and rate-limiting step operate in both channeling action and bulk reactions using mixed powders of carbon and catalysts. The results on channeling also indicate that the active intermediates are catalysts in the form of particles and clusters, and that the C–O–M (where M denotes metal) phenolate groups, although present in abundant amounts, are not the active intermediates. For very small particles, the surface free energy appears to play a role in lowering the amounts of CO_2 and H_2O chemisorbed, hence decreasing the channeling rates.

INTRODUCTION

Much attention has been attracted to the behaviors and catalytic actions of catalysts (metals, metal oxides, and salts) in the gas–carbon reactions. The gasification reactions of carbon by CO_2 (to form CO) and H_2O (to form H_2 and CO), in particular, are the bases for coal gasification, catalyst regeneration, and other chemical and metallurgical processes. For these two reactions, the alkali and alkaline earth salts are the best catalysts (see reviews (*1–5*). Much progress has been made during the past 2 decades toward the understanding of the mechanisms of these catalyzed reactions (*6–12*), possible active intermediates (*13–18*), and phenomena involved in the catalyst behaviors (*19–23*).

A generally postulated mechanism (*8, 10–12, 14*) consists of the oxidation–reduction cycle in which oxygen is transferred to the carbon active sites through the catalytically active alkali and alkaline earth species, followed by the liberation of C(O) from the carbon structure (by breaking the neighboring C–C bonds). The last step is considered as rate-limiting. This mechanism accounts for many experimental results, e.g., the similarity between activation energies of catalyzed and uncatalyzed reactions (*24–28*) and the rapid exchange of oxygen atoms between the gas phase (CO_2 and H_2O) and the catalysts (*7, 13, 21–24, 29, 30*). However, uncertainties remain concerning the active intermediates.

Many active intermediates have been proposed. Among all alkali and alkaline earth salts, potassium is the most extensively studied (due to its practical importance). The proposed active intermediates for potassium include metallic K (*9*), K_2O (*9, 31, 32*), K_2O_2 (*30*), K–O–C (*6, 15–17, 33, 34*), K_2CO_3 (*9, 31*), and clusters (*16, 21, 22*). Similar complexes have also been suggested for other catalysts (*7, 9, 23*). The C–O–K

[1] To whom correspondence should be addressed.

0021-9517/92 $5.00

phenolate-type group, first observed by Mims, Pabst, and co-workers (*15, 16*), has been shown to exist in large amounts on carbon surfaces during gasification by a number of experimental techniques. This type of intermediate has received the most attention. The recent study by Meijer *et al.* (*20*) suggested that the active intermediate is in the form of clusters with varying sizes (depending on the K/C ratio) and that the clusters are anchored by phenolate groups to the carbon surface.

A different approach to studying the catalyzed gas–carbon reactions has been microscopy, progressing from optical microscopy (*35*) to various techniques of electron microscopies such as etch-decoration TEM (*36, 37*) and controlled-atmosphere TEM (*38*), and STM (*39*). Microscopy is particularly useful for studying the catalyzed gas–carbon reactions because of the unique and most intriguing phenomenon of motions of the catalyst particles (or clusters) which result in the catalytic activity. The major catalyst motions include: pitting (*1, 35*), deep layer (multi-graphite layer) channeling and edge recession (*3, 38*), and monolayer channeling (*40–43*). The monolayer (single graphite layer) channeling action, in particular, provides quantitative kinetic data (since the depth of the channel is defined) and has resulted in a better understanding of the catalyst actions. The monolayer channeling is a pervasive phenomenon occurring in all gas–carbon reactions (i.e., reactions with H_2, O_2, CO_2, and H_2O) and can contribute significantly to these reactions (*40–43*).

To date, it has appeared that the results from the TEM studies are not related to the voluminous results from the bulk studies, i.e., studies using carbon powders or particles such as described in Refs. (*1–34*). In this work, we studied the monolayer channeling of alkali and alkaline earth catalysts in the C–CO_2 and C–H_2O reactions. An effort was made to relate the channeling action results to the bulk study results, with particular attention to the mechanism and active intermediates for these catalytic reactions.

EXPERIMENTAL

The carbon used in this study was a natural single-crystal graphite from Ticonderoga, New York. This graphite was chosen for its well-defined crystalline structure and ability to be cleaved into specimens thin enough (700 to 1000 Å thickness) for TEM observation while maintaining a large single-crystal basal plane area. A detailed explanation of the techniques used to prepare the crystals for reaction, catalyst deposition, and subsequent gold decoration has been given elsewhere (*37, 41*).

The catalyst precursors used were all of puratronic grade supplied by Alfa products, (Danvers, MA) with purities well above 99.9%. The precursors used were $LiC_2H_3O_2 \cdot 2H_2O$, Na_2CO_3, $NaNO_3$, K_2CO_3, KNO_3, $Ca(C_2H_3O_2)_2 \cdot H_2O$, and $Ba(NO_3)_2$. The CO_2 and N_2, used for gasification and as a carrier, respectively, were of ultrahigh purity grade (99.999% minimum purity for both) and were subjected to further purification to remove traces of O_2. The catalysts were dispersed on the basal plane of graphite from aqueous solutions. The graphite sample was placed on a filter paper, on which the solution was dispensed. After air drying, the catalysts were dispersed on the basal plane as confirmed by microscopy.

The catalyst-deposited graphite was placed on a sapphire plate held in an alumina combustion boat. The boat was placed in a quartz tube furnace reactor. Prior to reaction, it was necessary to degas the basal plane in N_2 at 500°C overnight. After degassing, the temperature was raised to the desired reaction temperature and the gas was switched to CO_2 or H_2O. Pure CO_2 or water vapor saturated in N_2 was used for the reaction. The graphite sample was subsequently subjected to gold decoration and viewed in TEM.

The first series of experiments involved two types of control experiments. First, the catalyst-deposited samples were heated to

the reaction temperatures (up to 700°C) for various periods of time (up to 8 hr) in the purified N_2 carrier, and no channels were observed on the basal plane. Second, graphite samples without catalyst deposition were subjected to CO_2 or H_2O reaction under the same conditions, and, again, no channels were observed.

Five catalysts (Li, Na, K, Ca, and Ba) were studied. The catalytic behaviors of the same alkali metals from different precursors (KNO_3 and K_2CO_3, $NaNO_3$ and Na_2CO_3) were also compared.

For rate calculations only channels with both clearly defined beginnings and ends were used.

RESULTS AND DISCUSSION

Monolayer channeling refers to the gasification of carbon by catalyst particles through the action of carving channels one graphite layer deep on the basal plane. This catalyst action has been observed and studied for the $C-H_2$ reaction (*40*), $C-O_2$ reaction (*42*), and the reactions with CO_2 and H_2O (*43*). The manner by which the channel depth is verified to be indeed monolayer has been described in detail (*40*). The origins from which monolayer channels initiate are lattice vacancies on the graphite basal plane and monolayer steps (*40*). The driving force for particle movement is also understood; it is caused by wetting or the balance of interfacial tensions (*40*). Since vacancies were abundant on the natural graphite sample, many monolayer channels were observed in the reacted samples. That these channels were indeed monolayer was verified in the same manner as described previously (*40–43*).

Catalyzed Graphite–CO_2 Reaction

Graphite samples with alkali (Li, Na, and K) and alkali earth (Ca and Ba) metal salts deposited were exposed to 1 atm CO_2 for 8 hr. No monolayer channeling was observed at temperatures below 600°C. After exposure at 600°C, the catalysts exhibited different faceting behaviors. The alkali metal particles tended to be faceted, the most faceted being K, whereas the alkali earth particles showed no tendency of faceting. Representative TEM views are shown in Fig. 1 for Li, K, and Ba catalysts. Faceting of K was also observed after exposure in a water vapor atmosphere at 600°C (*44*). K particles were present in sharp hexagonal forms. The faceted particles were oriented along the arm-chair of $\{11\bar{2}0\}$ directions of the graphite substrate, as indicated by electron diffraction of the graphite. Li particles exhibited only slight faceting. The faceting may be attributed to the anisotropic force field of the graphite basal plane. The carbon atom density along the arm-chair $\{11\bar{2}0\}$ direction is higher by approximately 20% than that along the zig-zag $\{10\bar{1}0\}$ direction. Consequently, the interactions between the catalyst and the substrate were stronger along the arm-chair direction, which resulted in the faceting of the particles. While the exact compositions of the particles were not known, the lower melting points of the alkali metal compounds (e.g., carbonates and oxides) caused them to exhibit a liquid-like behavior at 600°C (in CO_2). It was also observed that for both alkali and alkaline earth catalysts, the particles were dispersed preferentially along steps and defects on the graphite, caused by stronger interactions at these locations.

As the temperature was increased to above 650°C, the particles of all catalysts began to carve monolayer channels. Representative results are shown in Fig. 2 for K, Ca, and Ba catalysts reacted at 650° for 6 hr. Channeling by all different catalysts exhibited similar behaviors except their rates. Different precursors (carbonate and nitrate) of K and Na yielded the same results. The origins for monolayer channeling can be either vacancies of monolayer steps on the graphite basal plane; the channels shown in Figs. 2A and 2C were initiated at vacancies, whereas those in Fig. 2B were from a monolayer step (which was also shown by gold nuclei decoration). For the alkali and alkaline earth catalysts, the channeling direc-

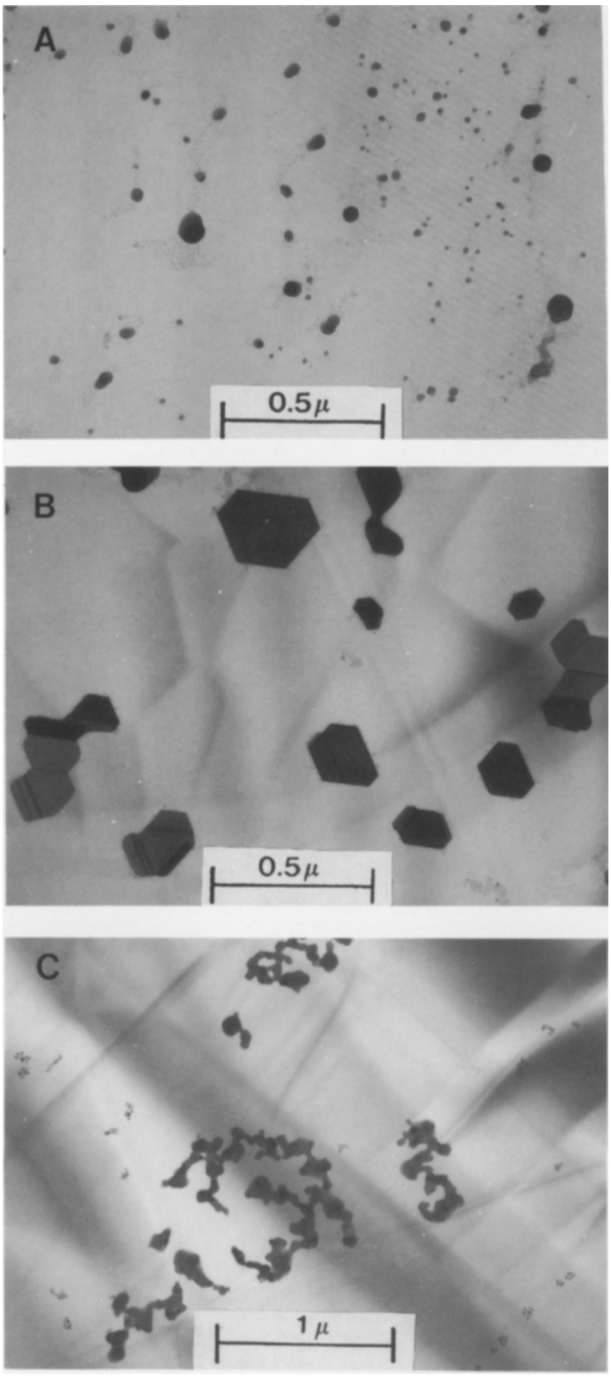

FIG. 1. TEM pictures showing the dispersion of carbonates of (A) Li, (B) K, and (C) Ba on the graphite basal plane after exposure to 1 atm CO_2 at 600°C for 8 hr.

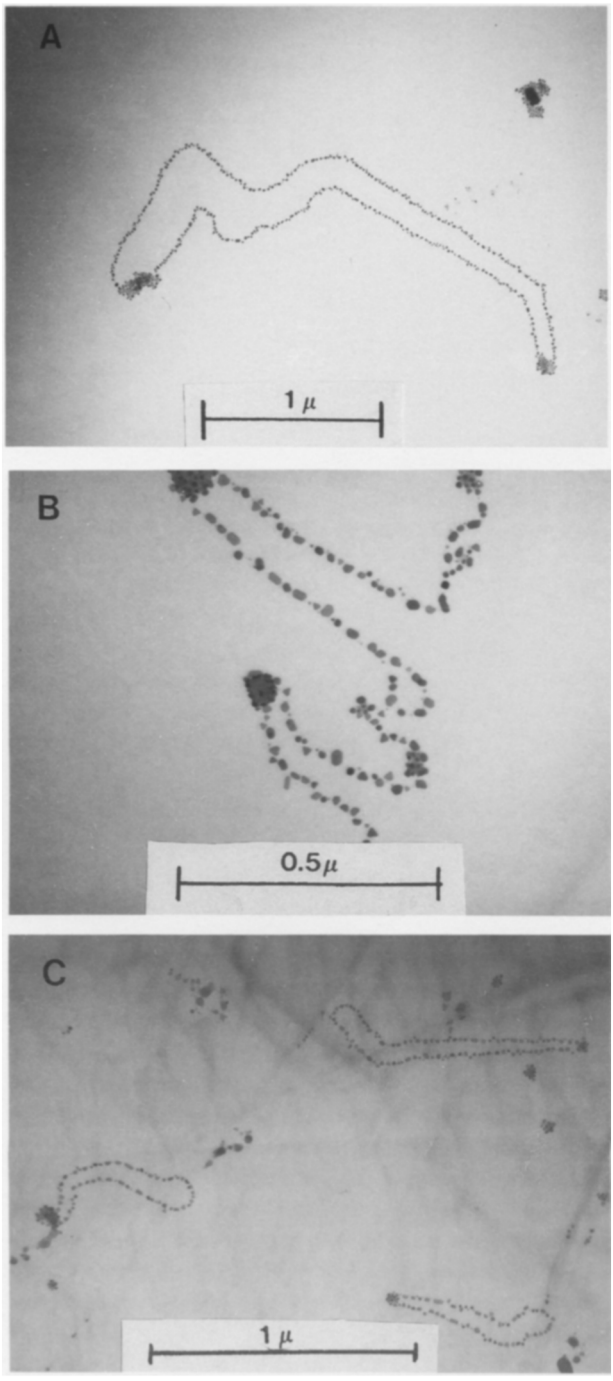

FIG. 2. TEM pictures of monolayer channels (decorated by gold nuclei) carved on the graphite basal plane by catalysts of (A) potassium, (B) calcium, and (C) barium after reaction in 1 atm CO_2 at 650°C for 6 hr.

TABLE 1

Turnover Frequency (Carbon Atom/Carbon Atom/s) by Different Catalysts

System	T(°C)	Li	Na	K	Ca	Ba
C–CO_2 (1 atm)	650	0.24 ± 0.05	0.31 ± 0.06	1.3 ± 0.1	0.45 ± 0.09	0.72 ± 0.2
C–H_2O (21 Torr)	690	3.1 ± 0.55	5.2 ± 0.2	8.5 ± 0.4	5.8 ± 0.2	7.2 ± 0.5

tions were random, and particles also changed directions as the channels propagated. The fact that all alkali and alkaline earth catalysts began to exhibit appreciable channeling activities at the same temperature suggests that the same reaction pathway was followed. This is in agreement with the results from bulk studies (using carbon powders) which suggested that alkali and alkaline earth catalysts only increased the concentration of the active complexes on carbon rather than changing the reaction pathway (*24–28*). The reaction was studied at both 650 and 700°C, but similar results were obtained.

By measuring the lengths of the monolayer channels which had both clearly defined beginnings and ends, the rates were calculated. Here the rates were expressed as turnover frequencies based on the active sites of carbon. The active sites were clearly defined, since they were located at the front leading edge of the catalyst particle. The turnover frequencies for the five different catalysts are listed in Table 1. These data are based on averages of at least five channels (each with clearly defined beginning and end) for each catalyst. The sizes of the particles used in the data ranged from 0.1–0.3 μm. The activities follow the rank: K > Ba > Ca > Na > Li. This same rank order has also been obtained from bulk kinetic studies using carbon powders (such as activated carbon) in flow or TGA reactors (*45–48*).

Catalyzed Graphite–H_2O Reaction

The monolayer channeling was studied for the five alkali and alkaline earth metal catalysts at 650 and 690°C in a gas atmosphere containing 21 Torr H_2O.

Similar to the catalyzed C–CO_2 reaction, no channeling was observed at temperatures below 600°C. At 600°C, however, very low channeling activities could be observed after prolonged reaction time (>10 hr) and by using high TEM magnifications. Vigorous channeling activities were observed at higher temperatures. The main features of the channeling are essentially the same as those in the C–CO_2 reaction. Figure 3 shows representative channels developed at 650°C after 2 hr reaction by Li and Ca particles. The turnover frequencies for the catalyzed C–H_2O reaction are also listed in Table 1. These data, like in the graphite/CO_2 system, are also based on averages of at least five channels for each catalyst. The turnover frequencies were, again, based on active sites of carbon. The rank order of the activities for the five catalysts is K > Ba > Ca > Na > Li, the same as in the C–CO_2 reaction.

Rate-Limiting Step for Monolayer Channeling

For both deep-layer channeling and monolayer channeling the following sequential steps are involved (*42*): (1) chemisorption and reaction of the gas molecule (O_2, CO_2, or H_2O) at the catalyst-gas interface, (2) transport (diffusion) of oxygen ions/atoms through or over the catalyst particle to the catalyst–carbon interface to form bonding with the edge carbon atoms, and (3) breakage of carbon–carbon bonds to free the edge carbon to release CO.

Goethel and Yang (*42*) has discussed in detail the rationale for determining the rate-

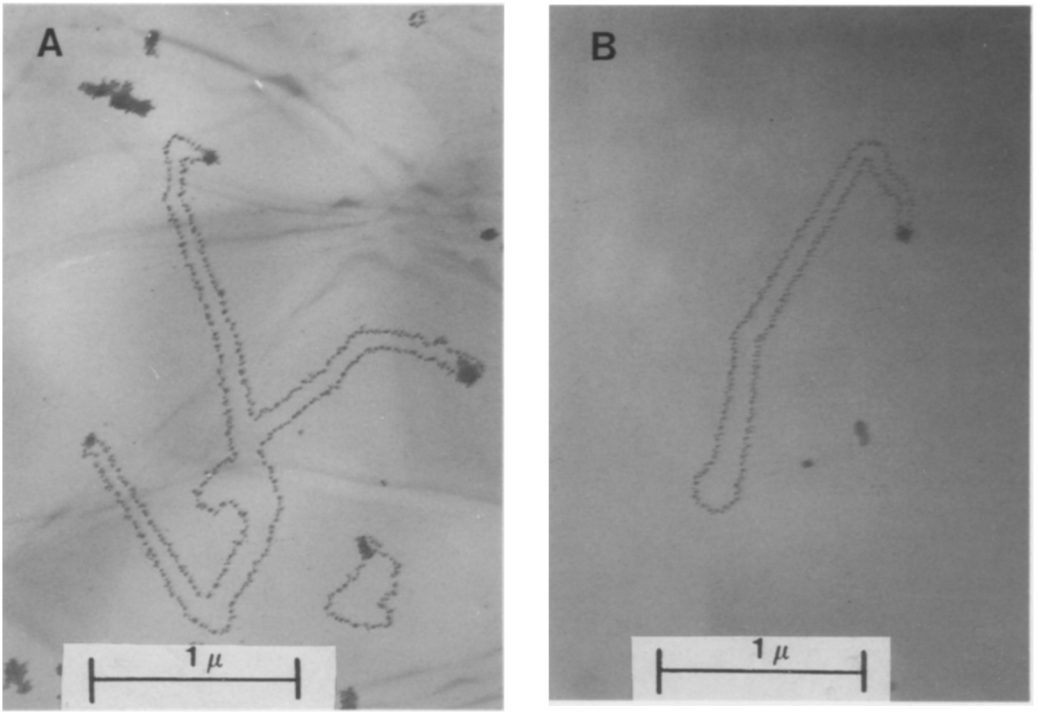

FIG. 3. TEM pictures of monolayer channels (decorated by gold nuclei) carved on the graphite basal plane by catalyst particles of (A) Li and (B) Ca after reaction in 21 Torr H_2O at 650°C for 2 hr.

limiting step based on the dependence of channeling rate on the particle size of the catalyst. The results for the alkali and alkaline earth catalyzed C–CO_2 and C–H_2O reactions showed a lack of dependence of the channeling rate on the particle size, except for very small sizes. A typical relationship between rate and size is shown in Fig. 4 for C–H_2O reaction catalyzed by potassium at 690°C. For particles smaller than a certain size, the channeling rate increased with the particle size. For the K/graphite/H_2O system (Fig. 4), the size threshold was approximately 750 Å, and for the K/graphite/CO_2 system, the threshold was 600 Å.

The independence of channeling rate on particle size (beyond the threshold) indicates that the rate-limiting step was the breakage of C–C bonds at the carbon–catalyst interface located at the advancing front of the catalyst particle. This conclusion is in agreement with the conclusion obtained

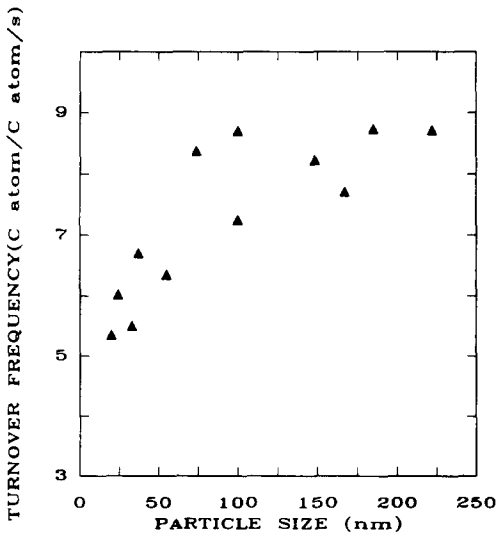

FIG. 4. Dependence of monolayer channeling rate on particle size for the K/graphite/H_2O (21 Torr) system at 690°C.

from bulk carbon studies. Isotope exchange experiments (*7, 13, 21–24*) showed that oxygen exchanges between gas reactant molecules (CO_2 and H_2O) and alkali metal catalysts were much faster than the carbon gasification rates, hence the C–C bond breakage was the rate-limiting step.

The rate-limiting step for the transition metal oxide (V_2O_5) catalyzed C–CO_2 and C–H_2O reactions is however, quite different (*43*). In these reactions, the channeling rate increases linearly with particle size, and the rate-limiting step is chemisorption (oxidation) at the surface of the catalyst (to raise the oxidation step by oxygen transfer) (*43*). The reason for the different rate-limiting steps is that the transition metal oxides are not as active as the alkali and alkaline earth compounds in the chemisorption of CO_2 and H_2O, which is essential for O atom transfer. Consequently, transition metals are not good catalysts for the C–CO_2 and C–H_2O reactions.

Behavior of Small Particles

As mentioned, for particles smaller than certain sizes, the channeling rates increased with size (Fig. 4). In order to interpret this result, one needs a further understanding of the rate-limiting step. (Conversely, this result will shed light on the rate-limiting step.)

From the bulk studies reported in the literature on the alkali catalyzed C–CO_2 and C–H_2O reactions, it is concluded that these catalysts only increase the concentration of the C(O) complex on the carbon surface, hence the overall rates (*24, 25, 27, 28*). The rate-limiting step being C–C bond breakage for channeling is consistent with this conclusion, since the C–C bond breakage is assisted by the O atom concentration at the edge carbon site.

The concentration of the C(O) complex will increase if the partial pressure of CO_2 or H_2O in the gas phase is increased, because more CO_2 or H_2O will be chemisorbed on the catalyst surface. The chemical compositions of the alkali species are not known and are dependent on the partial pressure, temperature, and dispersion. Moreover, within each particle, the composition varies, being more reduced toward the catalyst–carbon interface and more oxidized toward the gas–catalyst interface. For simplicity in this discussion, one may assume the following equilibria to dominate at the gas–catalyst interface: $K_2CO_3 = CO_2 + K_2O$ and $2KOH = H_2O + K_2O$.

For very small particles (or droplets, as the particles exhibit liquid-like behavior), the surface free energy (or surface tension) plays an important role in the vapor–liquid equilibria. The relationship is given below (a detailed discussion and experimental proof for the Kelvin equation are available in Adamson (*49*). The alkali oxide/carbonate equilibria should also be influenced by surface free energy for small sizes, and the Kelvin equation is used for our interpretation,

$$\ln \frac{P}{P_s} = \frac{2\sigma V_m}{rRT}, \qquad (1)$$

where P_2 is the partial pressure over a flat surface, P is equilibrium partial pressure over a particle with radius r, σ and V_m are the surface tension and molar volume of the particle, respectively, R is the gas constant, and T is the absolute temperature.

For our reactions with different particle sizes, the vapor pressure of CO_2 or H_2O is fixed. Therefore, the corresponding concentration of carbonate or hydroxide on the solid surface will be lower for smaller particles, via the Kelvin equation. For a constant vapor pressure, C_s is the surface carbonate concentration in the solid corresponding to flat surfaces (or large particles) and C is that over small particles, the Kelvin equation can be epxressed as (assuming Henry's law region of the Langmuir isotherm)

$$\ln \frac{C}{C_s} = -\frac{2\sigma V_m}{rRT}. \qquad (2)$$

For decreasing particle size, the chemisorption of CO_2 or H_2O decreases, which

in turn decreases the active C(O) complex concentration, hence lowers the channeling rate.

An estimate for the reduction of carbonate concentration by small sizes is given as follows: $T = 950$ K, $r = 300$ Å, and $V_m = 50$ cm^3/ml (for CO_2) and 20 cm^3/mol (H_2O). The surface tensions for alkali and alkaline earth metal oxides/carbonates at the reaction temperature are on the order of hundreds, e.g., $\sigma = 300$ dyne/cm. Using these values, Eq. (2) yields

$$\text{For } CO_2: \quad \frac{C}{C_s} = 0.77.$$

$$\text{For } H_2O: \quad \frac{C}{C_s} = 0.90.$$

These ratios are in qualitative agreement with the ratios of the channeling rates.

Similar size dependence has also been observed for other catalysts, except with differences in the threshold particle size and the plateau rate.

Shape of Channels: Relative Rates by C–O–K and Particles (Clusters)

Much research has been done to show the existence of the C–O–M phenolate-type groups (where M is alkali or alkaline earth metal) under carbon gasification conditions. These groups were first proposed by Mims, Pabst, and co-workers (*15, 16*) to be the active species of alkalies in the catalyzed reactions. The C–O–K group was shown to exist at 720 to 1000 K by ^{13}C-NMR (*15*) and methylation by CH_3I (*16*). It was found that about $\frac{1}{4}$ of the K atoms formed C–O–K and the fraction decreased with the K/C ratio (*16*). Using FTIR, Yuh and Wolf (*17*) also showed the existence of the C–O–K group for the C–H_2O reaction at 750°C. The C–O–M group as an intermediate has also been proposed by others (*45, 50*). More recently, the C–O–K group is suggested as the anchor for the catalyst clusters to attach to the edge carbon sites (*20, 34*). Whether the C–O–M group is the reactive intermediate, however, is an unresolved question. Insight into this question can be gained from the shape of the monolayer channels.

A very interesting picture observed in studying the monolayer channeling is that all channels carved by alkali and alkaline earth catalysts have a fluted appearance (e.g., Figs. 2 and 3). This phenomenon was not observed for the monolayer and deep-layer channeling in these reactions catalyzed by transition metal oxides, where all channels persisted with the same widths as the channels proceeded (*42, 43*). The fluted shape was also noted by Baker *et al.* (*51*) in their study of deep-layer channeling by barium in the C–H_2O reaction. They interpreted the observation by the deposition or coating of the catalyst on the channel walls and consequently the particle diminished in size which resulted in the fluted shape of the channel. This interpretation would not explain the fluted shape for monolayer channels.

The uncatalyzed carbon gasification is too slow to cause widening of the channel walls under the reaction conditions (*37*). The fluted shape indicates that a catalytic species exists on the channel walls, and that this species has a small activity. The published literature (*15–17*) suggests that the C–O–M group existed on the channel walls under our experimental conditions. Thus, the fluted shape of the channels would provide a good estimate for the ratio of the activity of the particle (or cluster) over that of the C–O–M group. The length of the channel represents the activity of the particle, whereas the amount of the widening of the channel represents the activity of the C–O–M group.

Estimates of the ratio of channel length/widening for the K-catalyzed monolayer channeling (in both CO_2 and H_2O reactions) yielded values in the range of 30 to 50. Thus, on a turnover frequency (per carbon active site) basis, the K particle is 30 to 50 times more active than the C–O–K group. Catalyst loss by evaporation and

coating on the channel walls undoubtedly also contributed to the fluted shape. Considering this factor, the actual ratio would be higher than 30–50.

Mechanism and Active Complex: Relating Channeling and Bulk Studies

From the voluminous literature on bulk studies (using bulk carbon) of catalyzed carbon gasification, the mechanism is similar to that for channeling. A unified mechanism involves the steps (using CO_2 as the reactant, H_2O replaces CO_2 in the first step to form H_2 for the C–H_2O reaction)

$$CO_2 + * \leftrightarrows CO + O^* \quad (3)$$

$$\text{Diffusion of } O^* \quad (4)$$

$$O^* + C^* \leftrightarrows C(O) + * \quad (5)$$

$$C(O) \leftrightarrows CO, \quad (6)$$

where * denotes the active site on the alkali or alkaline earth catalyst surface. Step (4) is diffusion either on surface or in the bulk catalyst lattice for the O atom or anion to reach the active site of carbon, C*, which is an edge atom on the graphite layer. The compositions of the particles are not known and are likely nonstoichiometric compounds (*52–54*) through which oxide ion can be transferred.

From bulk study results, it has been suggested that only clusters have catalytic activities. The difference between the mechanism for channeling by particles and the mechanism involved in bulk carbon reactions (e.g., reaction of polycrystalline carbon) is in Step (4). For channeling, the O atom/anion must diffuse across the particle to the edge carbon site. However, the diffusion step is rapid, and as a result, the rate-limiting step is Step (6) for both channeling and bulk reaction.

As mentioned in the foregoing, it has been suggested that clusters or particles are anchored on the edge carbon sites through the C–O–M phenolate groups. If this is indeed the case, since the active carbon sites are covered by the particle in the channeling action, Step (6) can be expressed in a more exact manner,

$$\begin{aligned} &- C - C - O - K + O^* \rightarrow \\ &\quad - C - C(O) - O - K \rightarrow \\ &\quad\quad CO + - C - O - K, \end{aligned} \quad (6a)$$

where the carbon atom in the C–O–K group is actually bonded to two carbon atoms and both are broken in order to free CO. The reaction shown in Step (6a) can also contribute to the differences in the turnover frequencies for different alkali and alkaline earth metals (Table 1). Results from bulk studies indicate that these differences are caused by the different concentrations of O* (i.e., different equilibrium constants for Step (3)) generated by different catalysts. Neither of the two causes can be ruled out.

From the fluted shape of the channels, it is suggested that the C–O–M groups have a low but finite catalytic activity. Apparently the C–O–M group does not chemisorb and dissociate CO_2 or H_2O as efficiently as particles or clusters. The lack of a good activity by the C–O–M group is also consistent with the fact that a minimum but large amount of catalyst is needed (to be mixed with the carbon powder) before catalytic activities are observed (e.g., 19).

A final note may be made concerning the sizes of the catalyst particles or clusters. The sizes depend on the dispersion, which in turn, depends on the temperature and gas environment and more importantly, on the structure of the substrate carbon surface. Relatively large particles can exist on the basal plane of graphite; the largest sizes under conditions in this study were approximately 0.3 μm. The sizes are considerably smaller on polycrystalline and edge plane graphite surfaces. However, the same catalytic mechanism and the rate-limiting step are operative in both particle channeling action on the basal plane and bulk reaction with mixed powders of catalyst and carbon. When the catalyst loading is high or the dispersion poor, there may exist carbonate in the alkali catalysts (*21*) and calcium catalyst (*21, 55*). In these circumstances, however,

CO_2 is transferred from the bulk to the carbon active sites which is rate-limiting and consequently the catalyst is not efficiently used.

CONCLUSION

Alkali and alkaline earth metal catalyst particles cut monolayer channels on the basal plane of graphite to gasify carbon in the C–CO_2 and C–H_2O reactions. Above certain particle sizes (e.g., 600 Å for the K/C/CO_2 system at 650°C and 750 Å for the K/C/H_2O system at 690°C) the channeling rates are independent of particle size. This result along with previous results on channeling lead to the conclusion that the rate-limiting step for channeling is the C–C bond breakage at the carbon-catalyst interface located at the advancing front of the catalyst. For very small sizes, the channeling rate decreases as the size decreases. It is proposed that the surface free energy plays a role for these small particles in the gas (CO_2 or H_2O)-liquid/solid (carbonate or hydroxide) equilibria, where the concentration of CO_2 or H_2O in the particle decreases for smaller particles.

The channeling characteristics for all five catalysts are similar, and are also similar in both C–CO_2 and C–H_2O reactions. The catalyst activities follow the order: K > Ba > Ca > Na > Li. This is in agreement with the bulk study results published in the literature where mixed powders of carbon and catalysts are used.

Comparing the channeling results and bulk study results, it is apparent that the same catalytic mechanism and rate-limiting step are operative in both channeling and bulk reaction.

The channels cut by alkali and alkaline earth catalyst particles exhibit a unique fluted appearance, which is not observed for other catalysts such as V_2O_5. Since the channel walls are covered by C–O–M phenolate-type groups, this result indicates that the C–O–M groups has a small activity but only particles and clusters have large activities, and it is the latter which contribute to the catalytic reactions.

ACKNOWLEDGMENT

This work was supported by NSF Grant CTS-9120452.

REFERENCES

1. Walker, P. L., Jr., Rusinko, F., Jr., and Austin, L. G., *in* "Advances in Catalysis," Vol. 11, p. 133. Academic Press, New York, 1959.
2. Wood, B. J., and Sancier, E. M., *Catal. Rev. Sci. Eng.* **26,** 233 (1984).
3. Baker, R. T. K., *in* "Carbon and Coal Gasification-Science and Technology" (J. L. Figuereido and J. A. Mulijn, Eds.), Martinus Nijhoff, NATO ASI Series E, No. 105, p. 231. Kluwer, Dordrecht, 1986.
4. Wen, W. Y., *Catal. Rev. Sci. Eng.* **22,** 1 (1980).
5. McKee, D. W., *in* "Chemistry and Physics of Carbon" (P. L. Walker, Jr., and P. A. Thrower, Eds.), Vol. 16. Dekker, New York, 1981.
6. Delannay, F., Tysoe, W. T., Heinemann, H., and Somorjai, G. A., *Carbon* **22,** 401 (1984).
7. Saber, J. M., Kester, K. B., Falconer, J. L., and Brown, L. F., *J. Catal.* **109,** 329 (1988).
8. Holstein, W. L., and Boudart, M., *J. Catal.* **75,** 337 (1982).
9. McKee, D. W., *Fuel* **62,** 170 (1983).
10. Radovic, L. R., Walker, P. L., Jr., and Jenkins, R. G., *J. Catal.* **82,** 382 (1983).
11. Moulijn, J. A., Cerfontain, M. B., and Kapteijn, F., *Fuel* **63,** 1043 (1984).
12. Mims, C. A., and Pabst, J. K., *J. Catal.* **107,** 209 (1987).
13. Chang, J., Lauderback, L. L., and Falconer, J. L., *J. Catal.***122,** 10 (1990).
14. Chang, J., Lauderback, L. L., and Falconer, J. L., *Carbon* **29,** 645 (1991).
15. Mims, C. A., Rose, K. D., Memchior, M. T., and Pabst, J. K., *J. Am. Chem. Soc.* **104,** 6887 (1982).
16. Mims, C. A., and Pabst, J, K., *Fuel* **62,** 176 (1983).
17. Yuh, S. J., and Wolf, E. E., *Fuel* **62,** 252 (1983).
18. Freriks, I. L. C., van Wechem, H. M. H., and Stuiver, J. C. M., *Fuel* **60,** 463 (1981).
19. Meijer, R., van der Linden, B., Kapteijn, F., and Moulijn, J. A., *Fuel* **70,** 205 (1991).
20. Meijer, R., Weeda, M., Kapteijn, F., and Moulijn, J. A., *Carbon* **29,** 929 (1991).
21. Cerfontain, M. B., Meijer, R., Kapteijn, F., and Moulijn, J. A., *Carbon* **26,** 41 (1988).
22. Saber, J. M., Falconer, J. L., and Brown, L. F., *J. Catal.* **90,** 65 (1984).
23. Chang, J., Adcock, J. P., Lauderback, L. L., and Falconer, J. L., *Carbon* **27,** 593 (1989).
24. Kelemen, S. R., and Freund, H., *J. Catal.* **102,** 80 (1986).
25. Freund, H., *Fuel* **65,** 63 (1986).
26. Pereira, P., Csencsits, T., Somorjai, G. A., and Heinemann, H., *J. Catal.* **123,** 463 (1990).

27. Kapteijn, F., Peer, O., and Moulijn, J. A., *Fuel* **65,** 1371 (1986).
28. Freund, H., *Fuel* **64,** 657 (1985).
29. Cerfontain, M. B., Meijer, R., Kapteijn, F., and Moulijn, J. A., *J. Catal.* **107,** 173 (1987).
30. Saber, J. M., Falconer, J. L., and Brown, L. F., *Fuel* **65,** 1356 (1986).
31. Veraa, M. J., and Bell, A. T., *Fuel* **57,** 194 (1978).
32. McKee, D. W., and Chatterji, S., *Carbon* **20,** 59 (1982).
33. Wood, B. J., Brittain, R. D., and Jai, K. H., *Prepr. Am. Chem. Soc. Div. Fuel Chem.* **28,** 55 (1983).
34. Gorrini, B. C., Radovic, L. R., and Gordon, A. L., *Fuel* **69,** 789 (1990).
35. Thomas, J. M., *in* "Chemistry and Physics of Carbon" (P. L. Walker, Jr., Ed.), Vol. 1. Dekker, New York, 1965.
36. Hennig, G. R., *in* "Chemistry and Physics of Carbon" (P. L. Walker, Ed.), Vol. 2. Dekker, New York, 1966.
37. Yang, R. T., *in* "Chemistry and Physics of Carbon" (P. A. Thrower, Ed.), Vol. 19. Dekker, New York, 1984.
38. Baker, R. T. K., *Catal. Rev. Sci. Eng.* **19,** 161 (1979).
39. Chu, X., and Schmidt, L. D., *Carbon* **29,** 1251 (1991).
40. Goethel, P. J., and Yang, R. T., *J. Catal.* **101,** 342 (1986).
41. Goethel, P. J., Ph.D. dissertation, State University of New York at Buffalo, Buffalo, NY, 1989.
42. Goethel, P. J., and Yang, R. T., *J. Catal.* **119,** 201 (1989).
43. Pan, Z. J., and Yang, R. T., *J. Catal.* **130,** 161 (1991).
44. Wong, C., and Yang, R. T., *Ind. Eng. Chem. Fundam.* **23,** 298 (1984).
45. Kapteijn, F., Porre, H., and Moulijn, J. A., *AIChE J.* **32,** 691 (1986).
46. Kapteijn, F., Abbel, G., and Moulijn, J. A., *Fuel* **63,** 1036 (1984).
47. Huhn, F., Klein, J., and Juntgen, H., *Fuel* **62,** 196 (1983).
48. Spiro, C. L., McKee, D. W., Kosky, P. G., and Lamby, E. J., *Fuel* **62,** 180 (1983).
49. Adamson, A. W., "Physical Chemistry of Surfaces," 3rd ed. Wiley, New York, 1976.
50. McKee, D. W., Spiro, C. L. Krosky, P. G., and Lamby, E. J., *Fuel* **62,** 217 (1983).
51. Baker, R. T. K., Lund, C. R. F., and Chludzinski, J. J., Jr., *J. Catal.* **87,** 255 (1984).
52. Holstein, W. L., and Boudart, M., *Fuel* **62,** 162 (1983).
53. Huttinger, K. J., and Minges, *Fuel* **65,** 1122 (1986).
54. Kapteijn, F., and Moulijn, J. A., *Fuel* **62,** 221 (1983).
55. Carzola-Amoros, D., Linares-Solano, A., Salinas-Martinez de Lacea, C., and Joly, J. P., *Carbon* **29,** 361 (1991).